Electronic Supplementary Material (ESI) for Journal of Materials Chemistry A.

Supporting Information for:

Solvent-Driven Responsive Bilayer Membrane of Clay and Graphene Oxide

*Raj Kumar Gogoi, Kundan Saha, Jumi Deka, Dulu Brahma and Kalyan Raidongia**
Department of Chemistry, Indian Institute of Technology Guwahati, Guwahati, 781039, Assam, India.
Email: k.raidongia@iitg.ernet.in

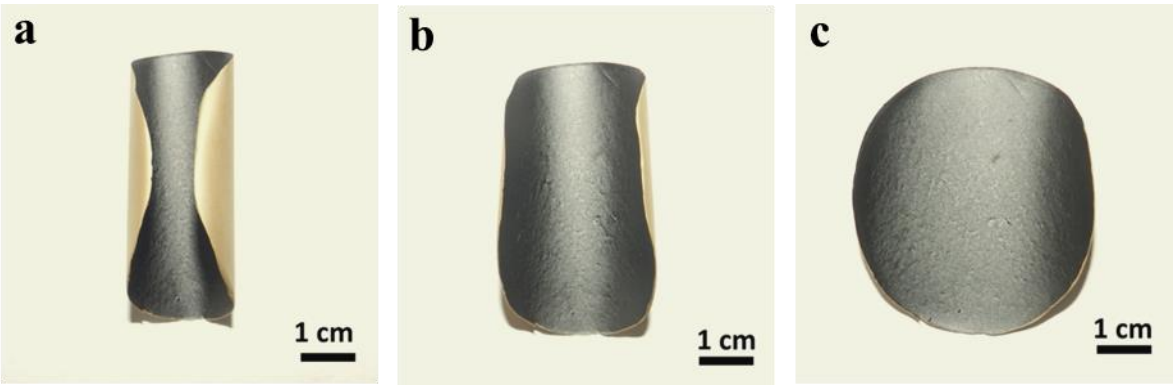

Figure S1: Humidity driven curling: Reversible curling of the clay-GO bilayer membrane as a function of relative humidity at 23 °C. (a) 78%. (b) 87% and (c) 95 % humidity.

Upon air-drying the clay-GO bilayer membrane tends to curl towards GO side. It could be due to the difference in water-holding capacity of the two components of bilayer membrane. While, GO membrane allows uninterrupted flows of water through its interlayer space,[1]vermiculite is famous for its extraordinary capacity to hold interstitial water molecules. Under open atmosphere, water molecules leaves GO fraction of the membrane initiating contraction of the same, while, on the other side, vermiculite layers hold them firmly. This one sided contraction develop asymmetric bending strain along the bilayer membrane leading to the curving of the same towards GO side. In order to prove this hypothesis, a curled membrane was stored in a high humidity (95 %) area, within 120 minutes the curled membrane opened-up by up taking of water molecules from atmosphere. This process was found to be highly reversible, as the same membrane kept in open atmosphere (78 % humidity) for 60 minutes leads to recovery of its original curved shape.

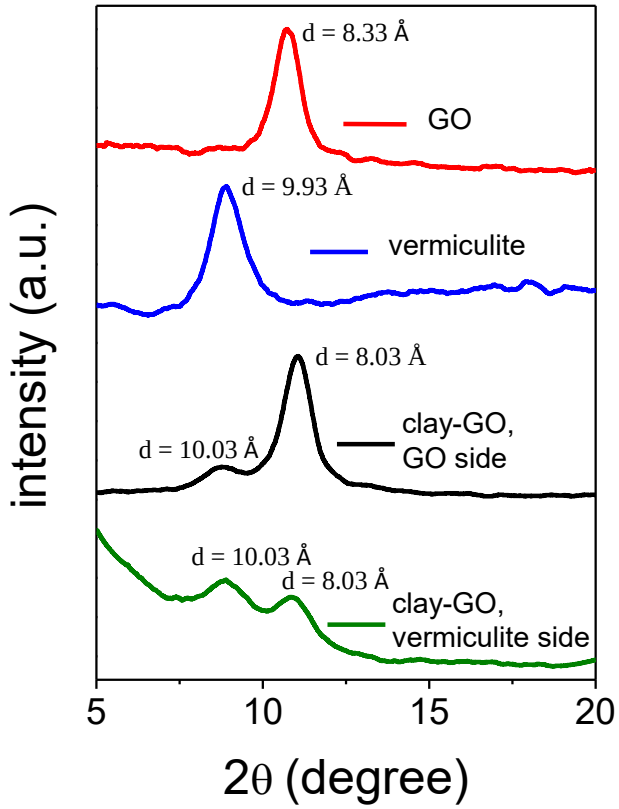

Figure S2: XRD patterns of membranes: XRD patterns of air dried GO, vermiculite and clay-GO bilayer membranes, exposing GO side and vermiculite side of the bilayer membrane.

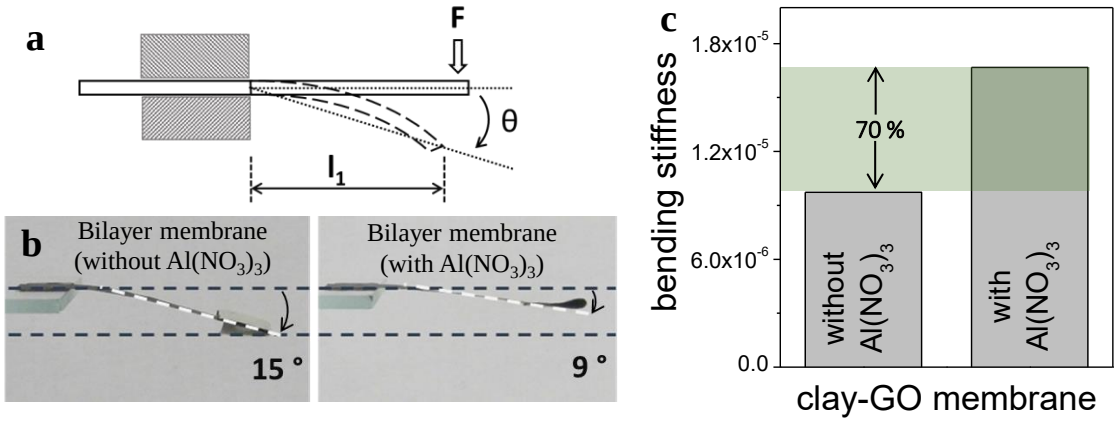

Figure S3: Bending stiffness of clay-GO bilayer membranes: (a) Schematic representation of bending stiffness measurements using 2 – point method. (b) Snapshots of the stripes of clay-GO bilayer membrane with load applied on the free end. (c) Comparison of the bending stiffness of the clay-GO membrane with and without addition of $Al(NO_3)_3$.

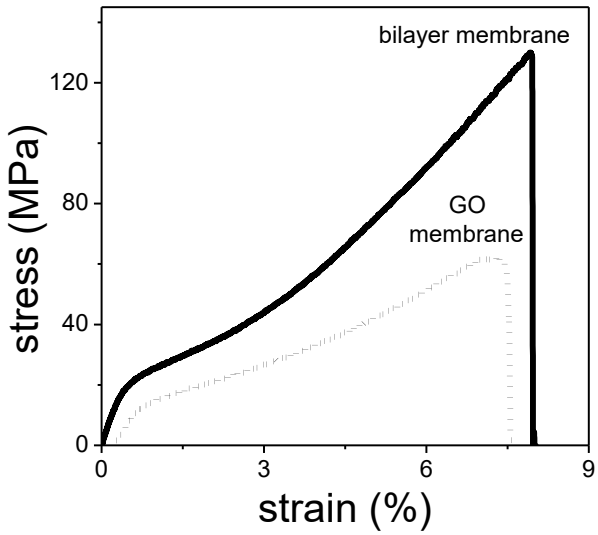

Figure S4: Stress-stain curve: Stress-stain curve of GO and clay-GO bilayer membrane (43 weight % of the GO membrane was replaced by vermiculite in the bilayer membrane).

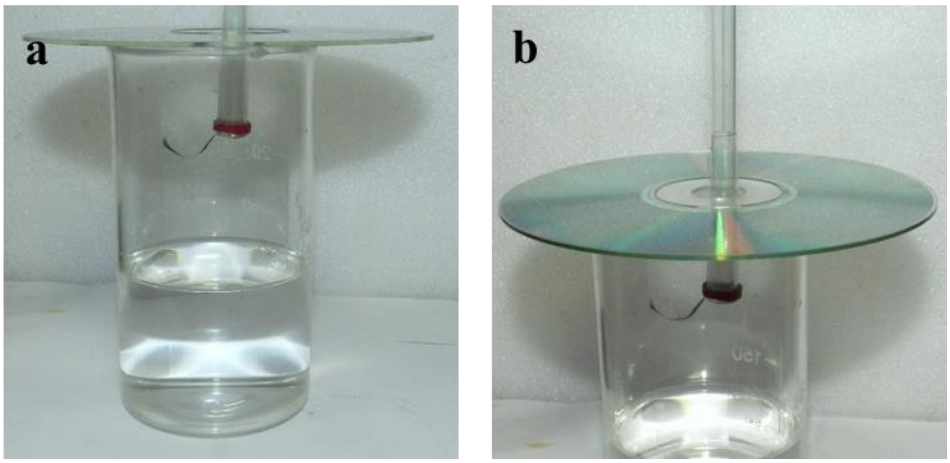

Figure S5: Experimental setup: Digital photos of the experimental setup utilized for the investigation of vapor stimulated bending properties of clay-GO bilayer membrane (a) side view and (**b**) top view of the experimental set up.

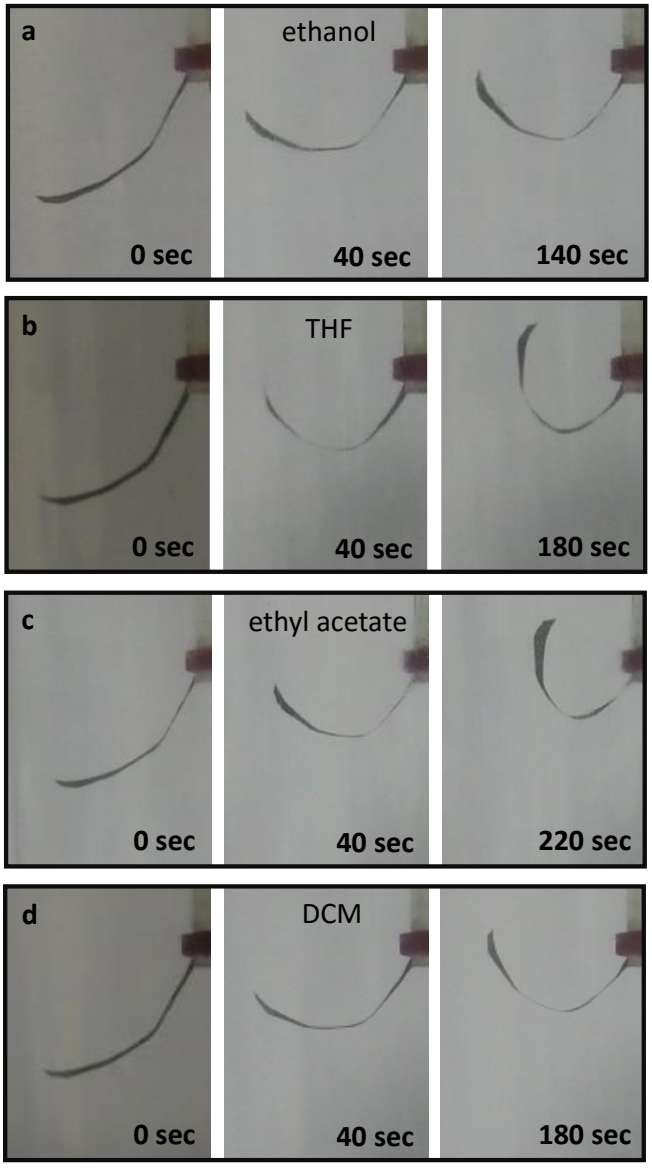

Figure S6: Vapor assisted bending: Snapshots of the bending movements of the bilayer stripe upon exposure to (a) ethanol, (b) THF, (c) ethyl acetate and (d) DCM.

Responsive behaviour of the bilayer stripe (dimension of 20 mm x 2 mm) was tested for ethanol, THF, ethyl acetate and DCM vapours. Similar to isopropanol, vapours of these solvents also stimulated additional bending of the stripe towards GO side. The bending and recovery speeds of the stripe stimulated by these solvents are shown in Figure 3d and 3e.

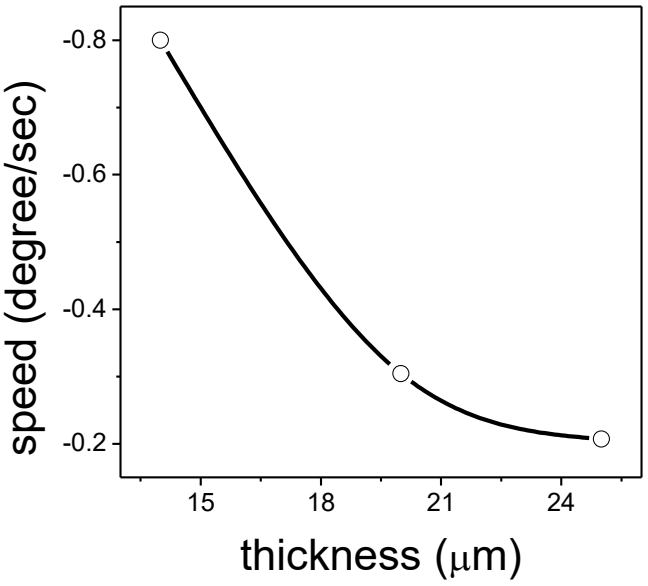

Figure S7: Effect of thickness on the bending speed of clay-GO bilayer stripe in presence of methanol vapor.

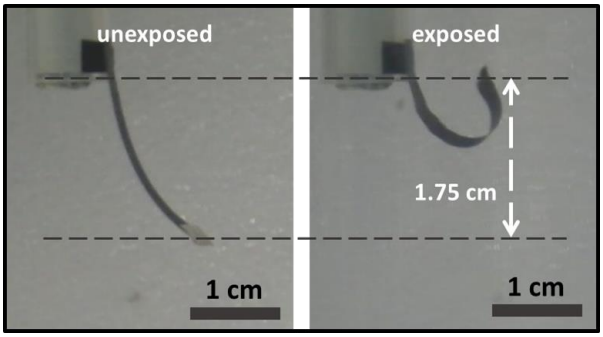

Figure S8: Work done by the bilayer stripe: Vapors assisted weight lifting by the bilayer stripe.

A stripe weighing 1.2 mg (dimension 20 mm × 2 mm), lifting 1.4 mg of weight up to 1.75 cm upon exposure to isopropanol vapors. The potential energy (*P.E.*) can be calculated using the relation $P.E. = m.g.h$

Where, m = weight, g = gravitational constant, h = height. The potential energy was calculated to be 2.4×10^{-7} J, with energy density of the stripe 2×10^{-4} J/g.

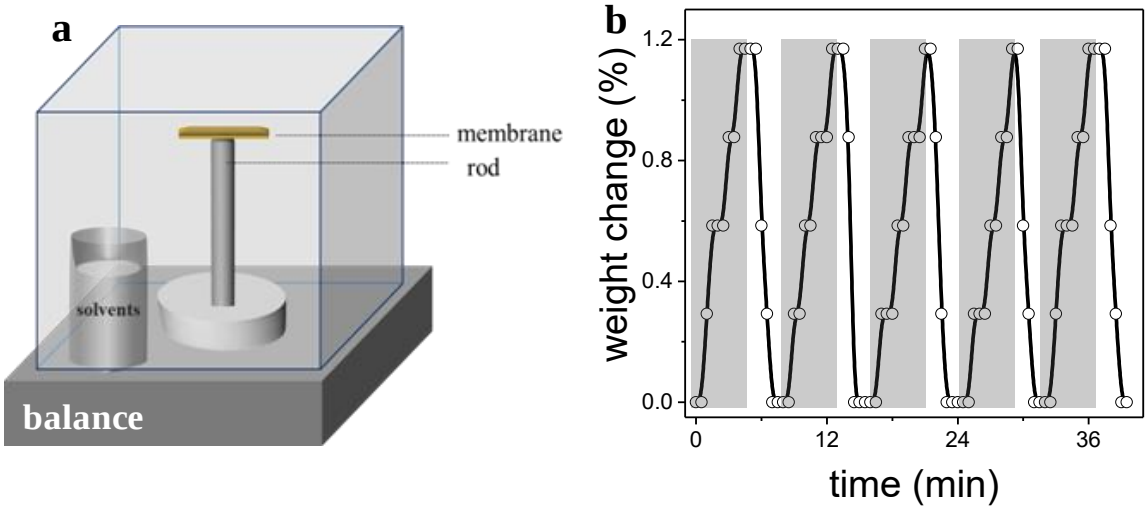

Figure S9: Reversible adsorption and desorption of solvent vapors by clay-GO bilayer membrane: (a) Semantic representation of the experimental setup used for measuring weight chance of the bilayer membrane. (b) Plot of weight changes versus time of the bilayer membrane during the process of adsorption and desorption of methanol vapor (weight increased portion of the curve shows adsorption of methanol and weight decreased part shows desorption of methanol in air atmosphere).

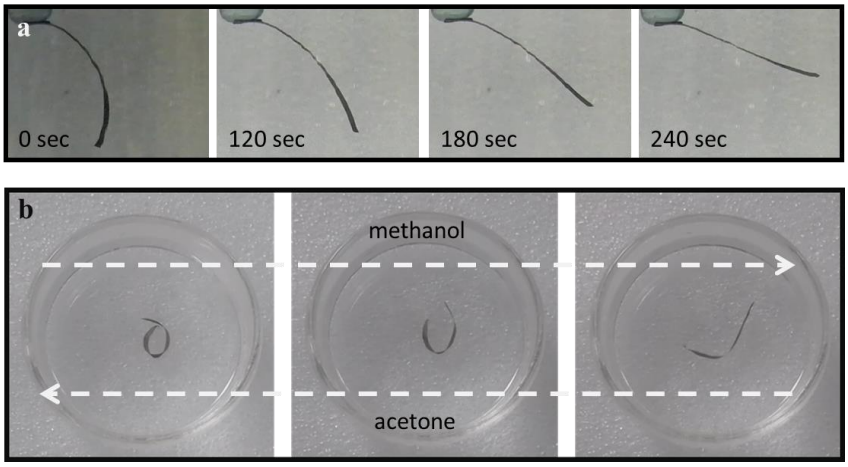

Figure S10, Responsiveness of bilayer membrane: (a) Bending of bilayer stripe against gravity in methanol environment. (b) Reversible curling and opening of the stripe in methanol-acetone system keeping both the ends unrestricted.

In order to confirm that the bending of the bilayer stripe in methanol vapor is not due to the effect of gravity on increasing weight of the stripe after adsorbing methanol, a stripe was exposed to methanol in a horizontal position. Suggesting, "bending" as an intrinsic property of the membrane, the bilayer stripe bent towards the vermiculite side against the gravity. The bilayer stripe can also be operated under liquid. A coiled stripe (20 mm x 2 mm, thickness 20 µm) cut from a membrane composed of 80 % GO and 20% vermiculite were dipped in methanol, the stripe opened-up instantaneously bending towards the vermiculite side. The initial coiled shape can be easily recovered by dipped it in to acetone.

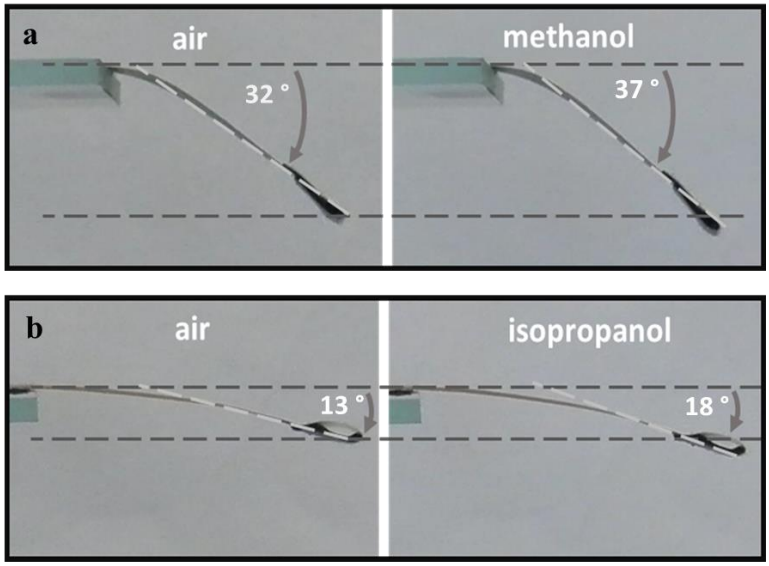

Figure S11: Vapor induced bending stiffness alteration of bilayer stripe: Snapshots of the stripes of (a) GO and (b) vermiculite with load applied on one end, before and after exposer to vapors.

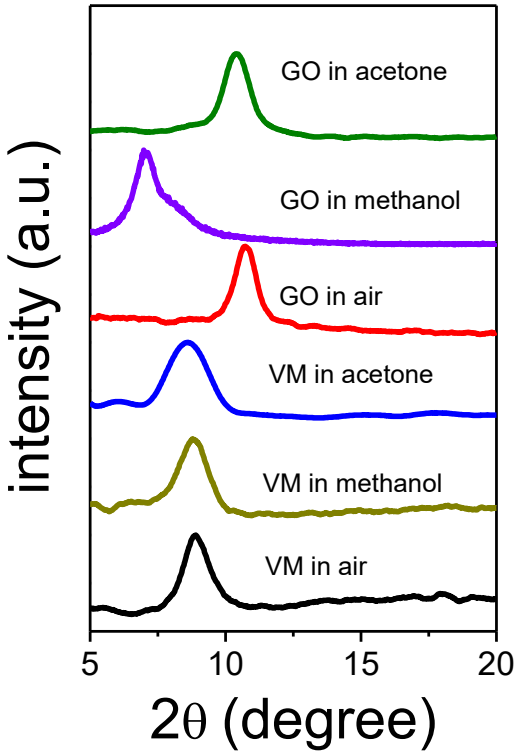

Figure S12: Alteration of interlayer spacing due to solvent intercalation: XRD patterns of air-dried GO and vermiculite membrane were compared with the one recorded after wetting the same with methanol and acetone solvents.

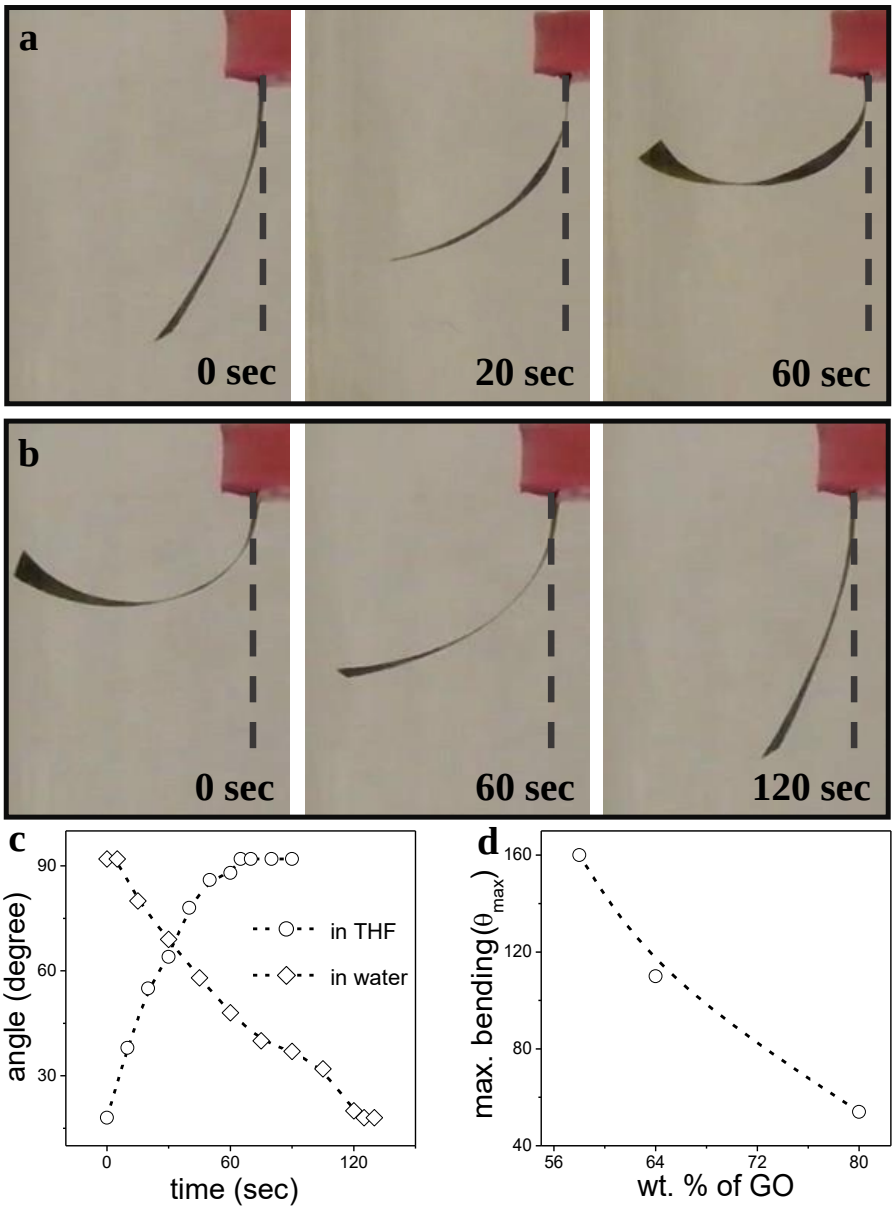

Figure S13: THF and water assisted bending of bilayer stripe: (a) Photos of bilayer stripe inside liquid THF after 0, 20, and 60 seconds of insertion. (b) Snapshots showing recovery of the bilayer stripe inside water at 0, 60, and 120 seconds. (c) Time versus bending angle plot in THF and water solvent. (d) Maximum bending of bilayer stripe in THF-water system as a function of GO content (weight %) in the membrane.

Stripe of GO-vermiculite bilayer membrane also responds to liquid THF and water by bending its shape. A bilayer stripe attached to a glass rod, "0 sec" image of Supporting Figure S8a, was immersed into a beaker of THF. The stripe instantaneously responded to THF molecules by

bending towards GO side and exhibits around 65 degrees of bending within 60 seconds. The bent stripe was then taken out of THF and dipped into water. In the contact with water, the bent stripe immediately started unfolding and became straight after around 120 seconds. The bending angle versus time curves for water and THF solvents are presented in Supporting Figure S8c. The speed of bending was found to be 1.10 degree/second and 0.58 degree/second for THF and water respectively. The solvent assisted reversible bending of bilayer membrane was repeatable at the same speed for four times after which the speed of bending decreases gradually. However, the original bending speed (0.5815 degree/sec) can be recovered by air-drying the membrane for 30 minutes. Bending in presence of water and THF were also tested with stripes of bilayer membranes prepared with different ratios of GO and vermiculite. A plot of maximum bending angle (θ_{max}) versus vermiculite fraction of the membrane is shown in Supporting Figure S8d. In contrast to methanol-acetone solvent pair, here responsiveness increases with decreasing GO content in the membrane.

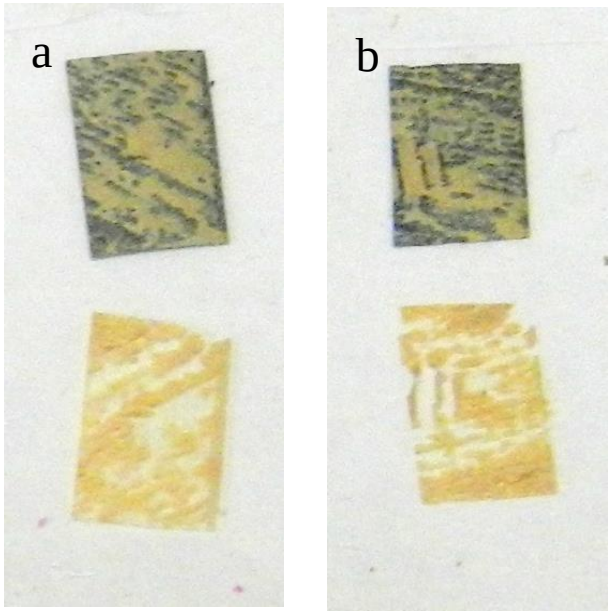

Figure S14: Digital photos of the interface of clay-GO bilayer membrane: The stability of the clay-GO interface was studied by peeling off a bilayer membrane with the help of adhesive tape. It is remarkable to see that the bilayer membrane did not get separated at the interface; instead, it was mostly separated at the vermiculite side of the membrane (a). Similar observation was also made with a bilayer stripe after repeating the solvent induced bending experiments for 25 times (b), suggesting the formation of a very stable GO-Clay interface.

Reference:

[1] R. R. Nair, H. A. Wu, P. N. Jayaram, I. V. Grigorieva and A. K. Geim, *Science*, 2012, **335**, 442-444.